Time Scales of Resonant Interactions Among Oceanic Internal Waves

C. HENRY MCCOMAS[1]

Woods Hole Oceanographic Institution, Woods Hole, MA 02543

PETER MÜLLER[2]

Harvard University, Cambridge, MA 02138

(Manuscript received 29 July 1980, in final form 3 November 1980)

ABSTRACT

Transfer rates and times of nonlinear resonant interactions within the oceanic internal wave field are evaluated analytically for the mechanisms which dominate the transfers within the Garrett-Munk spectral models (the elastic scattering, the induced diffusion, and the parametric subharmonic-instability mechanism). The analytic transfer rates assume that the interacting wave components are widely separated in wavenumber and/or frequency, and they are shown to agree well with the exact numerically calculated transfer rates. The analytic expressions are used to discuss conveniently and explicitly possible equilibrium states and the extent to which high-wavenumber internal waves can be treated in the weak-interaction limit. The Garrett-Munk spectral models are in equilibrium with respect to the elastic scattering, close to equilibrium with respect to the induced diffusion, and not in equilibrium with respect to the parametric subharmonic-instability mechanism. For an overall dissipation time scale of 30 days, waves with wavelength down to 5 m are weak.

1. Introduction

Nonlinear resonant interactions among oceanic internal waves are an important dynamical process, believed to determine the spectral shape of the internal-wave field and the efficiency by which internal waves diffuse mass and momentum. Nonlinear interactions redistribute energy and momentum among the various wave components. For a homogeneous, weakly interacting wave field the rate of change at a given wavenumber can be computed by using the random-phase approximation as a closure hypothesis; it is given by (Hasselmann 1966, 1967).

$$\frac{\partial}{\partial t}A(\mathbf{k}) = \int d^3k'd^3k''\{T^+\delta(\mathbf{k}-\mathbf{k}'-\mathbf{k}'')\delta(\omega-\omega'-\omega'') \times [A(\mathbf{k}')A(\mathbf{k}'')-A(\mathbf{k})A(\mathbf{k}')-A(\mathbf{k})A(\mathbf{k}'')] + 2T^-\delta(\mathbf{k}-\mathbf{k}'+\mathbf{k}'')\delta(\omega-\omega'+\omega'') \times [A(\mathbf{k}')A(\mathbf{k}'')+A(\mathbf{k})A(\mathbf{k}')-A(\mathbf{k})A(\mathbf{k}'')]\}, \quad (1)$$

where $A(\mathbf{k})$ is the action-density spectrum, $\mathbf{k}$ the wavenumber, $\omega = \omega(\mathbf{k})$ the frequency, and T^+ and T^- are transfer functions depending on $\mathbf{k}$, $\mathbf{k}'$ and $\mathbf{k}''$. Explicit expressions for the transfer functions are given by Müller and Olbers (1975) and Olbers (1976).

The transfer equation (1) can be interpreted in terms of two colliding wave or antiwave components creating or annihilating a third wave or antiwave component with collision cross sections T^+ and T^-. The δ functions assure that the collision process conserves momentum and energy.

The transfer integral has been evaluated by Olbers (1976) for the Garrett-Munk (1972, 1975) model spectra (henceforth, GM72 and GM75) and by McComas and Bretherton (1977, henceforth, MB) for the GM75 and GM76 (Cairns and Williams, 1976) model spectra. Olbers established the basic time scales of resonant nonlinear interactions in the energetic low-wavenumber part of the GM72 and GM75 spectra. MB extended the calculations to the higher shear-containing wavenumbers and, most importantly, discovered that much of the complex transfer can be understood in terms of three simple interaction mechanisms; the elastic scattering, the induced diffusion and the parametric subharmonic-instability mechanism. In a subsequent paper McComas (1977) showed that the GM spectra are in approximate equilibrium with respect to the induced-diffusion and elastic-scattering mechanisms and that small perturbations rapidly relax.

[1] Presently self-employed.

[2] On leave of absence from the University of Hamburg.

0022-3670/81/020139-09$06.25

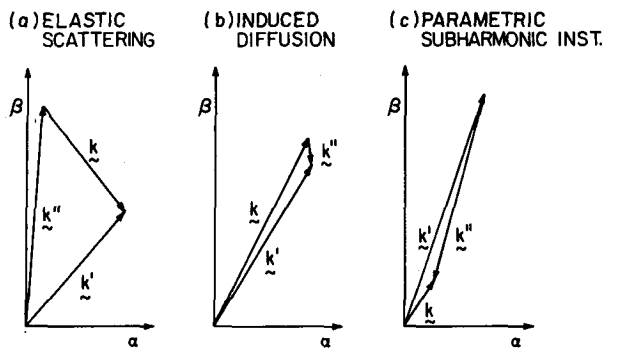

FIG. 1. Schematic representation of (a) elastic scattering, (b) induced diffusion and (c) parametric subharmonic instability triads.

Except for trivial spectra, the transfer integral in (1) has to be evaluated numerically. This requires considerable effort and care. Here we evaluate the transfer integral analytically for the three dominant transfer mechanisms by systematically exploiting the fact that the interacting wave components have largely different wavenumbers and/or frequencies for these mechanisms. The analytic approximations are shown to agree well with the "exact" numerically calculated transfer rates. We use the analytic expressions to discuss conveniently and explicitly the possible equilibrium states for these mechanisms and the question raised by Holloway (1980) as to what extent high-wavenumber internal waves can be treated in the weak interaction limit. The analytic approximations also provide a convenient tool to assess the dynamical role of nonlinear interactions in the energy balance of deep-ocean internal waves. This is more fully discussed by McComas and Müller (1981, abbreviated henceforth as MM).

2. Elastic Scattering

Elastic scattering denotes the vertical backscattering of a downward propagating, high-frequency wave $(\mathbf{k}', \omega')$ into an upward propagating, high-frequency wave $(\mathbf{k}, \omega)$ by a low-frequency near-inertial wave $(\mathbf{k}'', \omega'')$—see Fig. 1a. As in familiar Bragg scattering, the low-frequency component with twice the vertical wavelength, i.e., $k_3'' \sim 2k_3' \sim 2k_3$ is the most efficient scatterer. Elastic scattering transfers energy out of the more energetic of the high-frequency waves to the other, until their energies are equal. The low-frequency wave participates only weakly in the energy exchange, and can be considered as a given external field.

An analytic approximation to the transfer integral for this interaction process can be obtained by assuming $\omega, \omega' \gg \omega'' \approx f$ (f = Coriolis parameter) and $A(\mathbf{k}), A(\mathbf{k}') \ll A(\mathbf{k}'')$, and retaining only the lowest-order terms in an associated perturbation expansion. The first inequality is characteristic of the elastic-scattering mechanism; the second inequality is characteristic of the GM spectra, where most of the energy and action is concentrated at low frequencies. Under these assumptions the transfer integral is dominated by contributions from small horizontal wavenumbers $\alpha'' = 0$, and can adequately be approximated by setting $A(\mathbf{k}'') = \tilde{A}(k_3'')\delta(\alpha'')$. The transfer integral then reduces to

$$\frac{\partial}{\partial t} A(\mathbf{k}) = -\frac{A(\alpha, k_3) - A(\alpha, -k_3)}{2\tau(\mathbf{k})}, \qquad (2)$$

where

$$\tau^{-1}(\mathbf{k}) = 2 \sum_{\mu''=\pm} 2T^{\mu''} \frac{1}{|v_3(\mathbf{k})|} \tilde{A}(2k_3) \qquad (3)$$

or explicitly for $\omega^2 \ll N^2$ (hydrostatic limit)

$$\tau^{-1}(\mathbf{k}) = \tfrac{1}{4}\pi\omega N^{-2}\tilde{I}(2\beta) = \tfrac{1}{4}\pi\omega \,\mathrm{Ri}^{-1} \frac{\tilde{I}(2\beta)}{S}, \qquad (4)$$

where $\tilde{I}(\beta)d(\ln\beta) = f\beta^3\tilde{A}(\beta)d(\ln\beta)$ is the mean-square shear content in the logarithmic interval $d(\ln\beta)$, $S = \int_{-\infty}^{+\infty} \tilde{I}(\beta)d(\ln\beta)$ is the total mean-square shear, and Ri is the Richardson number N^2/S. Here β denotes the magnitude of the vertical wavenumber, $\mathbf{v}(\mathbf{k})$ the group velocity and N the Brunt Väisälä frequency.

The elastic scattering mechanism attenuates vertical asymmetries of the high-frequency wave field with the characteristic decay time τ. This decay time depends on the Richardson number and on the ratio of the shear content of the low-frequency scatterer to the total shear. Clearly, the smallest decay time possible is $\tau = 4\,\mathrm{Ri}\pi^{-1}\omega^{-1}$, when all the shear is at the length scale of the scatterer. We then find $\omega\tau = 4/\pi = O(1)$ for $\mathrm{Ri} = 1$. This is inconsistent with the weak-interaction limit which formally requires $\omega\tau \gg 1$. For the GM spectra, however, $\tilde{I}(\beta) \propto \beta^p$ with $p \in [\frac{1}{2}, 1]$ and $\beta \in [0, \beta_c]$, so that except for $\beta \sim \beta_c$ the weak interaction limit can be expected to be valid, even for such small Ri.

The dependence of τ on the vertical wavenumber β and the aspect ratio α/β (α = magnitude of horizontal wavenumber) is shown in Fig. 2 for the GM76 spectral model with $N = 5 \times 10^{-3}\ \mathrm{s}^{-1}$ and $f = 7 \times 10^{-5}\ \mathrm{s}^{-1}$. The Richardson number reaches one at β_c. The decay time decreases from a few days at low wavenumbers to a few minutes at high wavenumbers. Only at the very high wavenumbers does the transfer time become smaller than the period.[3]

Fig. 3 shows the relaxation time for the decay of a 10% perturbation to vertical symmetry in the GM76 spectrum, as obtained by evaluating the complete transfer integral numerically. Fig. 3 replaces Fig. 6 of McComas (1977), which is incorrect

[3] The shaded area depicts $\omega\tau \leq 1$. Since the period $\tau_p = 2\pi/\omega$ this region then formally corresponds to $\tau/\tau_p \leq (2\pi)^{-1}$.

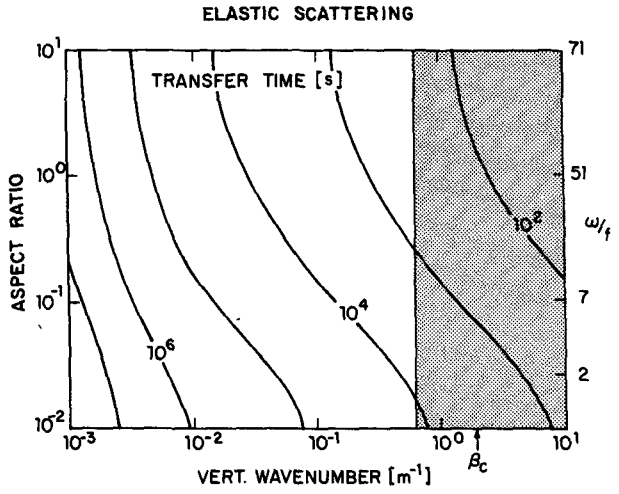

FIG. 2. Contour plot of the analytically calculated interaction time for the elastic scattering mechanism. This and the following plots have been evaluated for the GM76 spectral model with $N = 5 \times 10^{-3}\ s^{-1}$ and $f = 7 \times 10^{-5}\ s^{-1}$, corresponding to a latitude of 30°. The aspect ratio α/β is equivalent to a fixed frequency, as the internal wave frequency depends only on the wave number slope α/β. Lines of constant horizontal wavenumber are straight lines with a -1 slope. β_c is the cut-off wavenumber where the inverse Richardson number content becomes 1. In the shaded area the interaction time is smaller than the wave period.

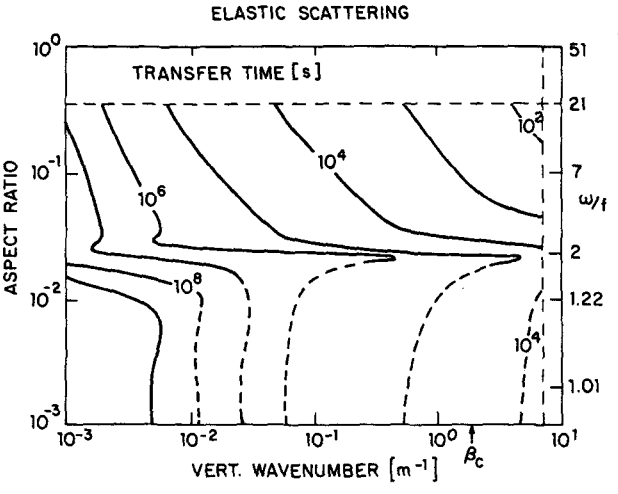

FIG. 3. Numerically calculated decay time of a 10% perturbation to vertical symmetry in the GM76 spectrum. Negative values (dashed) indicate that asymmetries grow.

because of a coding error. The agreement between our analytical approximation and the exact numerical calculation is good. Note that the analytical approximation is only valid for $\omega^2 \gg f^2$. The numerical calculation also shows that asymmetries of near-inertial oscillations do not relax. This is consistent with the observed asymmetry of near-inertial oscillations (Leaman and Sanford, 1975; Leaman, 1976; Müller *et al.* 1978).

The ratio $R'(\mathbf{k})$ of the numerically calculated decay rate of asymmetries and the numerically calculated transfer rate in the (vertically symmetric) GM76 spectrum is shown in Fig. 4 [which replaces McComas's (1977) Fig. 7]. This ratio highlights those regions in the spectrum where elastic scattering is a dominant process. The figure indicates that high-frequency waves are strongly affected by the elastic-scattering mechanism, whereas inertial oscillations are not.

The elastic-scattering mechanism describes the backscatter of high-frequency internal waves by low-frequency (inertial) currents. High-frequency waves also are backscattered by low-frequency density fluctuations, i.e., by the irreversible finestructure of the density stratification. This process has been studied by Mysak and Howe (1976) by decomposing the Brunt-Väisälä frequency into a mean component N^2 and a finestructure component δN^2. Again, a downward propagating high-frequency wave (α, k_3, ω) is scattered into an upward propagating wave $(\alpha, -k_3, \omega)$ by the Fourier component $2k_3$ of δN^2 (assumed to be horizontally uniform and time independent). In the hydrostatic limit $(\omega^2 \ll N^2)$ the decay rate of asymmetries is given by (Müller and Olbers, 1975)

$$\tau_{fs}^{-1}(\mathbf{k}) = \tfrac{1}{4}\pi\omega N^{-4}\tilde{F}(2\beta) = \tfrac{1}{4}\pi\omega C\tilde{F}(2\beta)/D, \quad (5)$$

where $\tilde{F}(\beta)\, d(\ln\beta)$ is the finestructure variance content in the logarithmic interval $d(\ln\beta)$, $D = \langle(\delta N^2)^2\rangle = \int \tilde{F}(\beta) d(\ln\beta)$ is the total variance of the finestructure, and C is the Cox number D/N^4 of the irreversible finestructure. The form of the decay time τ_{fs} closely resembles the form of τ, with density shear replacing current shear and the Cox number replacing the Richardson number. For typical mid-

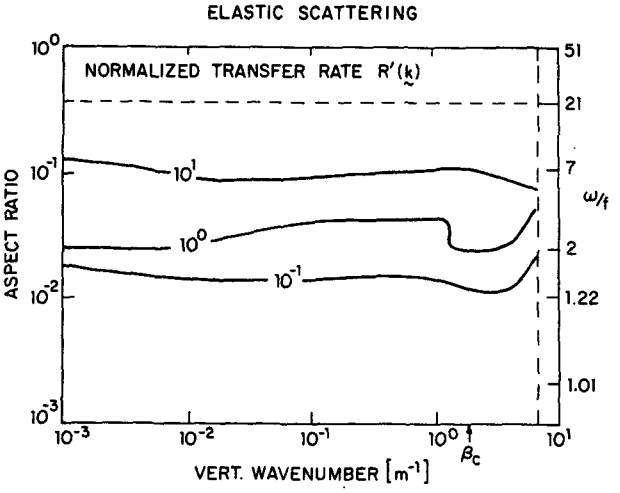

FIG. 4. Ratio of the numerically calculated decay rate of asymmetries to the numerically calculated interaction rate in the unperturbed GM spectrum.

ocean conditions current and density (temperature) spectra have similar vertical-wavenumber slopes and a comparable Richardson and Cox number ($\mathrm{Ri} \sim C \sim 1$). The two scattering processes are hence of comparable efficiency. A detailed comparison requires a model of the vertical wavenumber spectrum of the irreversible finestructure. This is not readily available from observations with temperature-profiling instruments that measure both the low-frequency irreversible finestructure and the reversible displacements of isotherms induced by high-frequency internal waves.

The elastic scattering at inertial currents and irreversible finestructure attenuates vertical asymmetries of the high-frequency wave field. The vertically symmetric GM spectral models are in equilibrium with respect to this process.

3. Induced diffusion

The scattering of a high-wavenumber, high-frequency wave ($\mathbf{k}$, ω) by a low-wavenumber, low-frequency wave ($\mathbf{k}''$, ω'') into another nearby high-wavenumber, high-frequency wave ($\mathbf{k}'$, ω') (Fig. 1b) leads to a diffusion of wave action (not wave energy) in wavenumber space. This result can be obtained either from a perturbation expansion (Fokker-Planck limit) of the transfer integral in Eq. (1) (Eisenschitz, 1958) or from a WKB approach using random-walk formulas (Taylor, 1921). The explicit form of the diffusion equation has been calculated by MB using both approaches and is given by

$$\frac{\partial}{\partial t} A(\mathbf{k}) = \frac{\partial}{\partial k_i} D_{ij} \frac{\partial}{\partial k_j} A(\mathbf{k}), \tag{6}$$

with the diffusion coefficient

$$D_{ij} = 2 \int d^3k' d^3k'' A(\mathbf{k}'') k_i'' k_j'' T^+ \times \delta(\mathbf{k} - \mathbf{k}' - \mathbf{k}'')\delta(\omega - \omega' - \omega''). \tag{7}$$

General scale analysis indicates that diffusion in vertical-wavenumber space is dominant. If we again approximate $A(\mathbf{k}'') = \tilde{A}(k_3'')\delta(\alpha'')$ the vertical diffusion coefficient becomes

$$D_{33} = \frac{1}{|v_3|}\left(\frac{f}{\omega}\right)^2 \tilde{A}\left(\frac{f}{|v_3|}\right) T^+ \tag{8}$$

or

$$D_{33} \approx \tfrac{1}{2}\pi\alpha^2 f^{-1} \tilde{I}\left(\frac{f}{\omega}\,\beta\right) \tag{9}$$

in the hydrostatic limit. Again, the near-inertial oscillations do not participate significantly in the energy exchange of the triad, and act like a given external field. Their shear content, however, determines the rate at which the diffusion takes place. The diffusion coefficient is independent of the vertical wavenumber only if the shear content is scale independent.

When calculating the characteristic time scale

$$\tau^{-1}(\mathbf{k}) = \frac{1}{A(\mathbf{k})} \frac{\partial}{\partial k} D_{33} \frac{\partial}{\partial k_3} A(\mathbf{k}) \approx \frac{D_{33}\Delta A}{(\Delta k_3)^2 A} \tag{10}$$

of the induced-diffusion mechanism, we must distinguish two cases. One time scale corresponds to the fastest possible time scale, which one obtains by choosing the maximum gradient, (i.e., $\Delta A/A \approx 1$ with $\Delta k_3 = k_3'' = f\omega^{-1}k_3$). This yields the fast time scale

$$\tau^{-1}(\mathbf{k}) = \tfrac{1}{2}\pi\omega N^{-2}\left(\frac{\omega}{f}\right)^3 \tilde{I}\left(\frac{f}{\omega}\,\beta\right) = \tfrac{1}{2}\pi\omega\,\mathrm{Ri}^{-1}\left(\frac{\omega}{f}\right)^3 \frac{\tilde{I}\left(\frac{f}{\omega}\,\beta\right)}{S}. \tag{11}$$

For the extreme case, $\mathrm{Ri} = 1$ and $\tilde{I}(f\omega^{-1}\beta)/S = 1$, we then find $\omega\tau = 2\pi^{-1}(f/\omega)^3$ if $\omega^2 \gg f^2$. Clearly, this strongly violates the condition for weak interactions as pointed out by Holloway (1980). Such a fast time scale is not unexpected, however. The fast time scale describes the decay of a spike in the spectrum. A spike represents a well-defined wavetrain with a large correlation length, many times its wavelength. Under random interactions such a wavetrain must be expected to deteriorate rapidly. With $\Delta A/A = 0.1$ the fast time scale (11) is shown in Fig. 5a; it corresponds to the numerical "bump" experiment of McComas (1977, Fig. 4), with which it favorably compares. Note again that the analytical approximation is only valid for $\omega^2 \gg f^2$.

However, for most spectra the actual gradient is not so large. In fact $\Delta A/\Delta k_3 \approx A/k_3$ is a more reasonable approximation for a smooth spectrum and it yields the slow time scale

$$\tau^{-1}(\mathbf{k}) = \tfrac{1}{2}\pi\omega N^{-2}\frac{\omega}{f}\tilde{I}\left(\frac{f}{\omega}\,\beta\right) = \tfrac{1}{2}\pi\omega\,\mathrm{Ri}^{-1}\frac{\omega}{f}\frac{\tilde{I}\left(\frac{f}{\omega}\,\beta\right)}{S}, \tag{12}$$

implying $\omega\tau = 2\pi^{-1}f/\omega \ll 1$ for the extreme case. This still violates the weak-interaction assumption but not so badly as before. And, for all GM spectra $\omega\tau \gg 1$ for $\beta \ll \beta_c$ and $\omega \gg f$, since $\tilde{I}(f\omega^{-1}\beta)/S \ll 1$. A contour plot of the slow time scale (12) as a function of β and α/β for the GM76 spectrum is shown in Fig. 5b.

Thus, the evolution of a smooth spectrum is adequately described by weak-interaction theory, but the evolution of a spiked spectrum is not!

So, is the wave field weak or strong? The proper answer depends on the sources and sinks within the

wave field. If the sources and sinks are weak, i.e., if their characteristic time scale $\tau_s(\mathbf{k})$ is much larger than the wave period, then the diffusion can keep up with the input, the gradients never become large, and the problem is adequately described by the weak interaction diffusion limit. If the sources and sinks are strong and highly localized in wavenumber space, however, causing steep gradients in the spectrum, then the problem is not weak and cannot be accurately evaluated using weak-interaction theory.

If we assume that dissipation acts like a vertical viscosity (MM, 1980) then

$$\frac{E(\mathbf{k})}{\tau_s(\mathbf{k})} = -\nu S(\mathbf{k}), \tag{13}$$

where the viscosity coefficient ν is determined by $E/30$ days $= \nu S$, such that the time scale for energy dissipation is 30 days. From (13) we find a dissipation time scale

$$\tau_s(\mathbf{k}) = \gamma\beta^{-2}, \tag{14}$$

where $\gamma = 2.5 \times 10^4$ s m^{-2} such that the wave field can be considered weak for vertical wavelengths > 5 m if Ri $= 1$ and $N = 5 \times 10^{-3}$ s^{-1}.

Are the GM spectral models in equilibrium with respect to the induced-diffusion mechanism? The diffusion equation has two equilibrium solutions: a no-flux solution with $A(\mathbf{k})$ independent of k_3, i.e., $A(\mathbf{k}) = F(\alpha)$; and a constant-flux solution with $D_{33}(\partial A(\mathbf{k})/\partial k_3)$ independent of k_3, i.e., $A(\mathbf{k}) = -Q(\alpha) \times \int (1/D_{33})dk_3$, where $Q(\alpha)$ is the flux. Only the constant-flux solution allows for dissipation at high wavenumbers. In general, the no-flux and constant-flux solutions will have different vertical-wavenumber dependencies. For the GM spectral models, a high-wavenumber slope $t = -2$ is the no-flux equilibrium solution at medium frequencies, $f^2 \ll \omega^2 \ll N^2$, and high wavenumbers, $\beta \gg \beta_*$ (β_* = wavenumber bandwidth).

A constant-action-flux equilibrium for high-frequency waves under the diffusion mechanism requires that there are no changes in the high-frequency portion of the spectrum, while action is moved to larger vertical wavenumbers at constant horizontal wavenumber, i.e., to lower frequencies. Because action is conserved by the diffusion, the energy content of the high-frequency region would decrease if not supplied by the inertial waves to maintain equilibrium. A constant action flux at the high frequencies requires an energy gain at the inertial frequencies. Thus, if the high-frequency portion of the spectrum is in a constant-flux equilibrium, then the low-frequency portion cannot be. MM (1980) argue that the vertical-wavenumber spectrum including both frequency ranges is in equilibrium under a constant *energy* flux.

In this paper, however, we take the inertial wave field as a given external field and consider only the equilibrium of the high-frequency internal waves. If the low-frequency vertical-wavenumber slope is $t = -2$ then $D_{33} \propto \beta^2$ and the high-frequency equilibrium slope is $t = -3$. If the low-frequency slope is $t = -2.5$ then $D_{33} \propto \beta$ and the high-frequency equilibrium slope is observationally indistinguishable from $t = -2$. A spectral slope of $t = -2$ at all frequencies is not an equilibrium solution in the presence of flux (and dissipation); however, a near-inertial slope of $t = -2.5$ and a high-frequency slope of $t = -2$ is near equilibrium in the presence of a flux and dissipation.

For a more accurate estimate of the diffusion time scale we consider the spectra

$$A(\mathbf{k}) = A_0 \frac{\beta}{\alpha}\frac{\omega}{N}\left(\frac{\omega}{N}\right)^{-4-p}\left(\frac{\beta}{\beta_*}\right)^{-4-p-q} \tag{15}$$

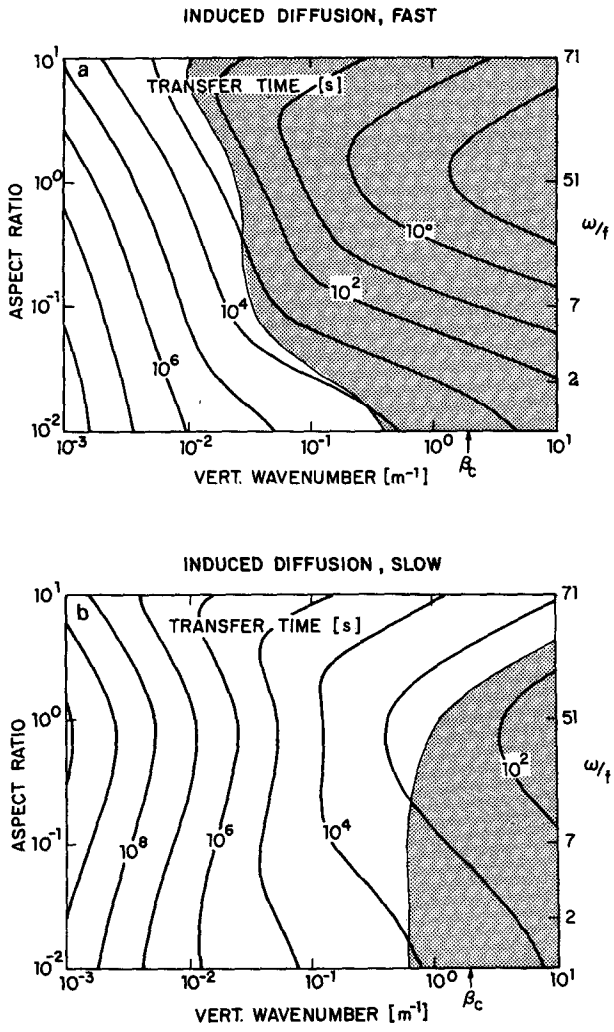

FIG. 5. Contour plot of the analytically calculated (a) fast and (b) slow induced diffusion time scale. In the shaded area the diffusion time scale is smaller than the wave period.

which approach

$$A(\mathbf{k}) = A_0\left(\frac{\omega}{N}\right)^{-4-p}\left(\frac{\beta}{\beta_*}\right)^{-4-p-q}$$

$$= A_0\left(\frac{\alpha}{\beta_*}\right)^{-4-p}\left(\frac{\beta}{\beta_*}\right)^{-q}$$

for $\omega^2 \gg f^2$ and are characterized by the high-wavenumber slopes p and q. The GM75 spectral model corresponds to $p = 0.0$, $q = 0.5$, and the GM76 model to $p = 0.0$, $q = 0.0$. The spectra with $q = 0$ and p arbitrary represent no-flux solutions, while the spectra with $p = (1 - 3q)/2$ represent constant-flux solutions. The diffusion rate for this class of spectra is

$$\tau^{-1}(\mathbf{k}) = \frac{1}{A(\mathbf{k})}\frac{\partial}{\partial k_3} D_{33} \frac{\partial}{\partial k_3} A(\mathbf{k})$$

$$= q(1 - 3q - 2p)\tfrac{1}{2}\pi\omega \frac{\omega}{f} \mathrm{Ri}^{-1} \frac{\tilde{I}\left(\frac{f}{\omega}\beta\right)}{S}, \quad (16)$$

which is just $R = q(1 - 3q - 2p)$ times the slow time scale (12). The factor R as a function of q and p is shown in Fig. 6. The two valleys correspond to the no-flux and constant-flux solutions. Under the action of the induced-diffusion mechanism spectra should evolve towards the equilibrium valleys unless held back by strong generation or dissipation mechanisms. Note that the induced-diffusion mechanism by itself forces spectra into the equilibrium valleys but not to a specific position within the valleys. This position is determined in conjunction with some other process (see MM, 1981).

To assess how well the induced-diffusion mechanism approximates the complete nonlinear transfer, we compare in Fig. 7 our analytically calculated diffusion rate (16) with the exact transfer rate obtained from a numerical evaluation of the complete transfer integral. Three cuts ($p = 0.5, 0.0$ and -0.5) through the p-q plane are shown. The solid curves represent the diffusion rate, and the points with the error bars the exact transfer rate, both normalized by the diffusion rate (12). The exact transfer rate is the mean rate obtained by averaging 4×3 estimates in the region $8\sqrt{2}f \leq \omega \leq 32\sqrt{2}f$ and $1/60\ \mathrm{m}^{-1} < \beta < 1/6\ \mathrm{m}^{-1}$. The error bars denote the standard deviation of this estimate. Also indicated are the ratios of standard deviation to mean value. No exact transfer rates have been calculated for $p = -0.5$ and $q \leq 0$ since spectra with high-wavenumber slopes $-1 - 2p - q > 0$ do not satisfy the condition for scale separation, on which our derivation of the diffusion equation is based.

Generally, the agreement between the diffusion and exact transfer rate is good, except close to the equilibrium valleys. Here the diffusivé transfer becomes small and other interactions become important. Close to the equilibrium valleys the exact transfer rates also show considerable scatter in the wavenumber-frequency plane, a further indication that the diffusion time scale is not appropriate.

4. Parametric subharmonic instability

The parametric subharmonic-instability mechanism denotes a transfer wherein a low-vertical-wavenumber wave ($\mathbf{k}$, ω) decays into two high-vertical-wavenumber waves ($\mathbf{k}'$, ω') and ($\mathbf{k}''$, ω'') of approximately half the frequency (Fig. 1c). This mechanism was identified by MB as causing the energy transfer from low to high wavenumber near inertial oscillations in the GM spectra. On the assumptions that $\beta \ll \beta'$, β'' and $\omega \sim 2\omega' \sim 2\omega'' \sim 2f$ with $A(\mathbf{k}')$, $A(\mathbf{k}'') \ll A(\mathbf{k})$, the transfer integral reduces to

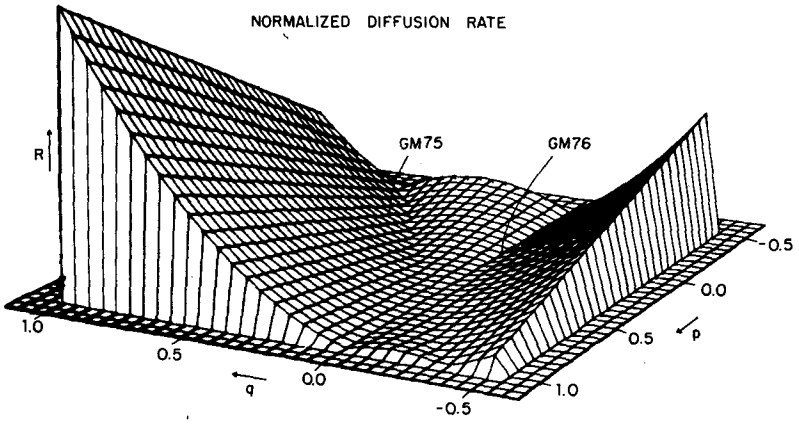

FIG. 6. Normalized diffusion rate as a function of the high wavenumber slopes p and q.

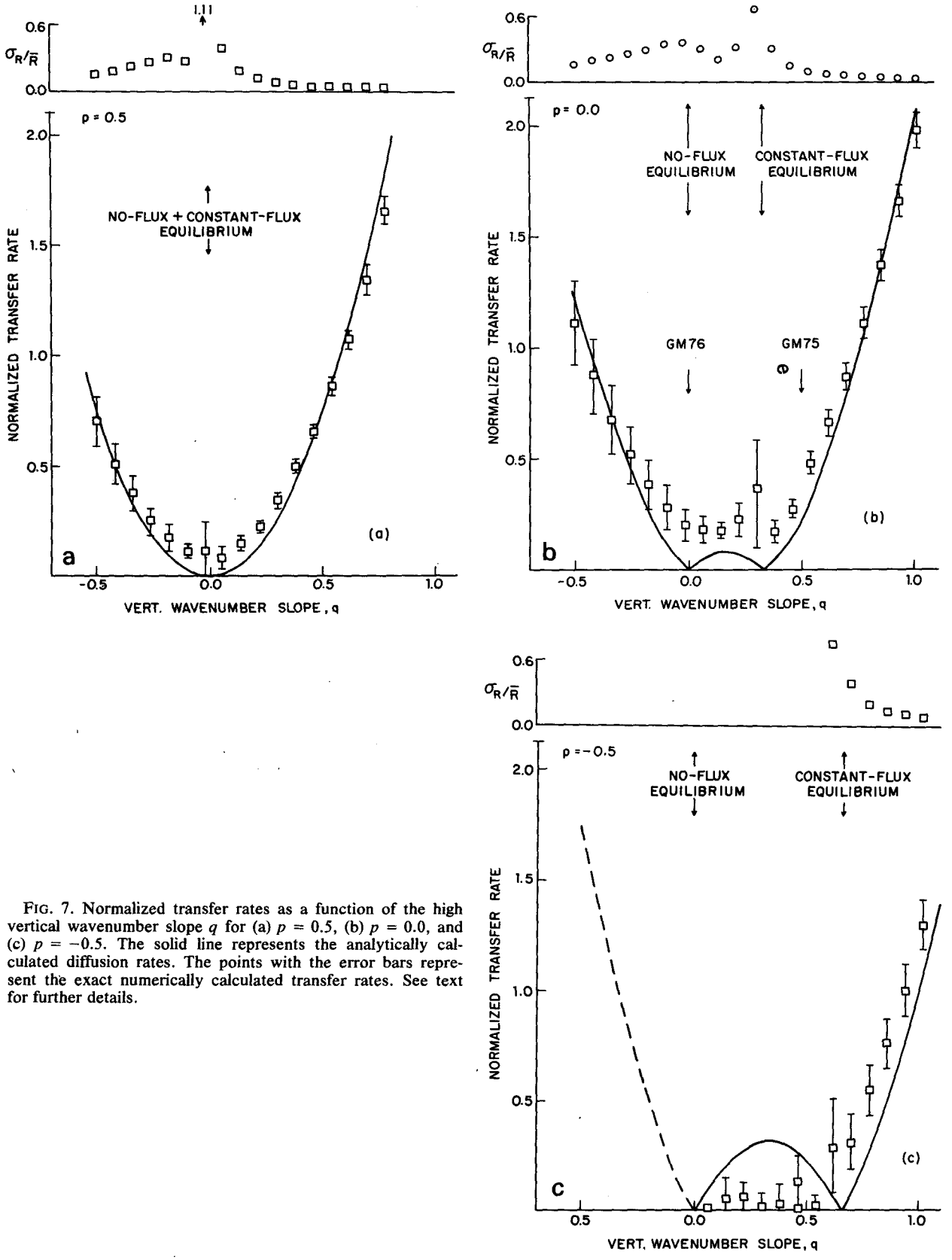

FIG. 7. Normalized transfer rates as a function of the high vertical wavenumber slope q for (a) $p = 0.5$, (b) $p = 0.0$, and (c) $p = -0.5$. The solid line represents the analytically calculated diffusion rates. The points with the error bars represent the exact numerically calculated transfer rates. See text for further details.

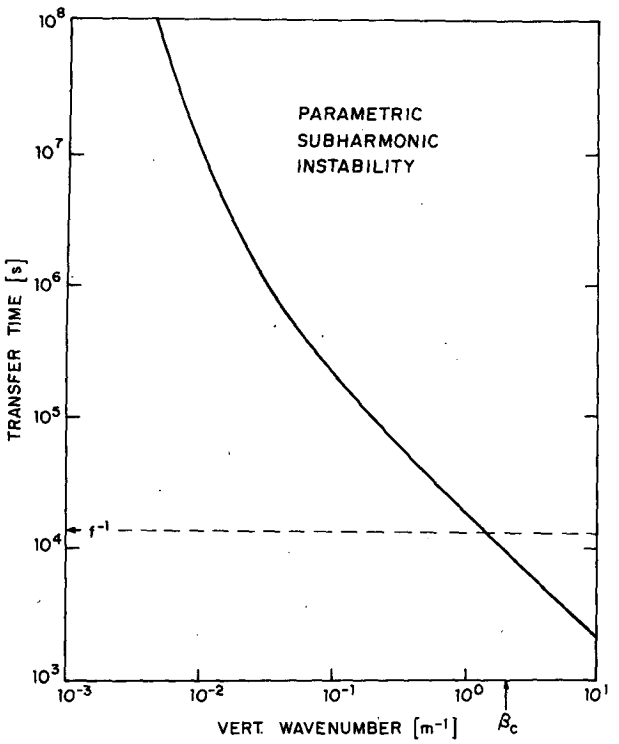

FIG. 8. Analytically calculated growth time of the parametric subharmonic instability mechanism as a function of vertical wavenumber.

$$\frac{\partial}{\partial t} A(\mathbf{k}) = -2A(\mathbf{k}) \int d^3k' T^+ \times \delta[\omega - \omega' - \omega(\mathbf{k} - \mathbf{k}')]A(\mathbf{k}') \quad (17)$$

for the loss at low wavenumbers, and to

$$\frac{\partial}{\partial t} A(\mathbf{k}') = 4A(\mathbf{k}') \int d^3k T^- \times \delta(\omega - \omega' - \omega(\mathbf{k} - \mathbf{k}'))A(\mathbf{k}) \quad (18)$$

for the gain at high wavenumbers. The transfer functions are given by

$$T^+ = T^- = \frac{9}{16} \pi f \alpha^2. \quad (19)$$

The parametric subharmonic-instability mechanism dominates the total transfer only at high wavenumbers (MB). There, the characteristic growth rate is explicitly given by

$$\tau^{-1}(\mathbf{k}') = \frac{27}{8} \pi \frac{f^2}{N^2} \tilde{I}\left(\frac{1}{x}\beta', 2f\right) = \frac{27}{8} \pi f^2 \, \mathrm{Ri}^{-1} \frac{\tilde{I}\left(\frac{1}{x}\beta', 2f\right)}{S}, \quad (20)$$

where

$$x = \left(\frac{3}{2} \frac{f}{\omega' - f}\right)^{1/2}. \quad (21)$$

The growth rate of the near inertial wave depends on the shear content of the double-frequency wave with a wavenumber x times smaller. The factor x arises because near inertial waves $(\mathbf{k}', \omega')$ can only be generated by double-frequency waves $(\mathbf{k}, \omega)$ with vertical wavenumbers $\beta \leqslant \beta'/x$, because of the resonance constraints. If we assume $\tilde{I}(\beta, \omega) = \tilde{I}(\beta) f/\omega^2$ the growth rate becomes

$$\tau^{-1}(\mathbf{k}') = \frac{27}{32} \pi f N^{-2} \tilde{I}\left(\frac{\beta'}{x}\right) = \frac{27}{32} \pi f \mathrm{Ri}^{-1} \frac{\tilde{I}\left(\frac{\beta'}{x}\right)}{S}. \quad (22)$$

The growth time (22) is shown in Fig. 8 for $x = \sqrt{10}$ (the average value of x for the GM spectral models) and compares favorably with the exact numerical calculation displayed in Fig. 11 of MB. Again, $\omega\tau^{-1} \gg 1$ except for $\beta \sim \beta_c$ and larger.

Equilibrium with respect to the parametric subharmonic-instability mechanism requires that the energy levels of the interacting waves be equal, i.e., $A(\mathbf{k}') \sim A(\mathbf{k}'') \sim 2A(\mathbf{k})$ or $E(\mathbf{k}') \sim E(\mathbf{k}'') \sim E(\mathbf{k})$. Partial equilibrium may be obtained by increasing the energy of inertial waves, i.e., an inertial peak. The GM spectra are not in equilibrium, however. Energy is still transferred from small to large wavenumbers.

The parametric subharmonic-instability mechanism and the induced-diffusion mechanism represent the low- and high-frequency limits of the transfer at high vertical wavenumbers. High-vertical-wavenumber waves with frequencies close to f interact mainly with a low-vertical-wavenumber wave of twice the frequency. This is the parametric subharmonic-instability mechanism. High-vertical-wavenumber waves with frequencies much larger than f interact mainly with a low-vertical-wavenumber, low-frequency wave. This is the induced-diffusion mechanism. In the intermediate frequency range the transfers are not dominated by any particular scale-selective interaction triad.

5. Conclusions

Nonlinear interactions transfer energy and momentum among the various wave components. The numerical evaluation of the transfer rates for the GM spectral models by McComas and Bretherton (1977) showed that the transfer at high frequencies and high wavenumbers is dominated by the induced-diffusion mechanism, at low frequencies and high

TABLE 1. Dimensionless transfer rates for the various interaction mechanisms.

	$(\omega\tau)^{-1}$, general	$(\omega\tau)^{-1}$, GM76
Elastic scattering	$\frac{\pi}{4}\,\mathrm{Ri}^{-1}\,\frac{\tilde{I}(2\beta)}{S}$	$\frac{E\beta_*^2}{N^2}\,\frac{\beta}{\beta_*}$
Induced diffusion, slow	$\frac{\pi}{2}\,\mathrm{Ri}^{-1}\,\frac{\omega}{f}\,\frac{\tilde{I}\left(\frac{f}{\omega}\beta\right)}{S}$	$\frac{E\beta_*^2}{N^2}\,\frac{\beta}{\beta_*}$
Induced diffusion, fast	$\frac{\pi}{2}\,\mathrm{Ri}^{-1}\left(\frac{\omega}{f}\right)^3\,\frac{\tilde{I}\left(\frac{f}{\omega}\beta\right)}{S}$	$\frac{E\beta_*^2}{N^2}\left(\frac{\omega}{f}\right)^2\,\frac{\beta}{\beta_*}$
Parametric subharmonic instability	$\frac{27}{8}\,\pi\,\mathrm{Ri}^{-1}\,\frac{f\tilde{I}\left(\frac{\beta}{x},2f\right)}{S}$	$\frac{27}{32\sqrt{10}}\,\frac{E\beta_*^2}{N^2}\,\frac{\beta}{\beta_*}$

wavenumbers by the parametric subharmonic-instability mechanism, and in an asymmetric high-frequency field by the elastic-scattering mechanism. The transfers within the energetic low-frequency, low-wavenumber region are weak and not dominated by any particular process. In this paper the transfer rates and times for the three dominant mechanisms were evaluated analytically. The analytical approximations utilized the specific relationships between the frequencies and wavenumbers of the interacting waves for each of the processes, and the fact that energy and action are concentrated at low frequencies and wavenumbers for the GM spectral models. The analytic approximations were shown to agree well with the exact numerically calculated transfer rates.

The analytically calculated transfer rates are listed in Table 1. They depend on the Richardson number and on the ratio of the shear content of the low-frequency near-inertial waves to the total shear. For the GM76 spectral model the transfer times are remarkably equal, except for the fast diffusion time scale.

The analytical approximations provide a convenient tool to discuss various dynamical problems. We specifically discussed as to what extent high-wavenumber internal waves can be treated in the weak-interaction limit. The internal wave field can be considered weak as long as the sources and sinks are weak. For an overall dissipation time scale of 30 days, waves with wavelengths down to 5 m are weak. We also discussed the possible equilibrium states. The GM spectral models are in equilibrium with respect to the elastic-scattering mechanism, close to equilibrium with respect to the induced-diffusion mechanism, and not in equilibrium with respect to the parametric subharmonic-instability mechanism. The full potential of the analytical approximations becomes evident when one attempts to solve the complete radiation-balance equation of the internal-wave field, including sources and sinks. Results are discussed by MM (1980).

Acknowledgments. This work has been supported by the National Science Foundation under Grant OCE77-25803 and by the Office of Naval Research under Contracts N00014-75-C-0225 and ONR N00014-76-C-0197. This is a contribution of the Sonderforschungsbereich 94, Meereskunde Hamburg and Contribution No. 4750 from the Woods Hole Oceanographic Institution.

REFERENCES

Cairns, J. L., and G. O. Williams, 1976: Internal wave observations from a midwater float. 2. *J. Geophys. Res.*, **81**, 1943–1950.

Eisenschitz, R., 1958: *Statistical Theory of Irreversible Processes*. Oxford University Press, 128 pp.

Garrett, C. J. R., and W. H. Munk, 1972: Space-time scales of internal waves. *Geophys. Fluid Dyn.*, **2**, 225–264.

——, 1975: Space-time scales of internal waves: A progress report. *J. Geophys. Res.*, **80**, 291–297.

Hasselmann, K., 1966: Feynman diagrams and interaction rules of wave-wave scattering processes. *Rev. Geophys. Space Phys.*, **4**, 1–32.

——, 1967: Nonlinear interactions treated by the methods of theoretical physics (with applications to the generation of waves by wind). *Proc. Roy. Soc. London*, **A299**, 77–100.

Holloway, G., 1980:Oceanic internal waves are not weak waves. *J. Phys. Oceanogr.*, **10**, 906–914.

Leaman, K. D., 1976: Observations on the vertical polarization and energy flux of near-inertial waves. *J. Phys. Oceanogr.*, **6**, 894–908.

——, and T. B. Sanford, 1975: Vertical energy propagation of inertial waves: A vector spectral analysis of velocity profiles. *J. Geophys. Res.*, **80**, 1975–1978.

McComas, C. H., 1977: Equilibrium mechanisms within the oceanic internal wave field. *J. Phys. Oceanogr.*, **7**, 836–845.

——, and F. P. Bretherton, 1977: Resonant interaction of oceanic internal waves. *J. Geophys. Res.*, **82**, 1397–1412.

——, and P. Müller, 1981: The dynamical balance of internal waves. Submitted to *J. Phys. Oceanogr.*

Müller, P., and D. J. Olbers, 1975: On the dynamics of internal waves in the ocean. *J. Geophys. Res.*, **80**, 3848–3860.

——, —— and J. Willebrand, 1978: The IWEX spectrum. *J. Geophys. Res.*, **83**, 479–500.

Mysak, L. A., and M. S. Howe, 1976: A kinetic theory for internal waves in a randomly stratified ocean. *Dyn. Atmos. Oceans*, **1**, 3–31.

Olbers, D. J., 1976: Nonlinear energy transfer and the energy balance of the internal wave field in the deep ocean. *J. Fluid Mech.*, **74**, 375–399.

Taylor, G. I., 1921: Diffusion by continuous movement. *Proc. London Math. Soc.*, **20**, 196–212.